

SUBMILLIMETER ARRAY OBSERVATIONS OF 321 GHz WATER MASER EMISSION IN CEPHEUS A

NIMESH A. PATEL¹, SALVADOR CUIEL², QIZHOU ZHANG¹, T. K. SRIDHARAN¹, PAUL T. P. HO^{1,3}, JOSÉ M. TORRELLES⁴

Draft version February 28, 2007

ABSTRACT

Using the Submillimeter Array (SMA) we have imaged for the first time the 321.226 GHz, $10_{29} - 9_{36}$ ortho- H_2O maser emission. This is also the first detection of this line in the Cepheus A high-mass star-forming region. The 22.235 GHz, $6_{16} - 5_{23}$ water masers were also observed with the Very Large Array 43 days following the SMA observations. Three of the nine detected submillimeter maser spots are associated with the centimeter masers spatially as well as kinematically, while there are 36 22 GHz maser spots without corresponding submillimeter masers. In the HW2 source, both the 321 GHz and 22 GHz masers occur within the region of $\sim 1''$ which includes the disk-jet system, but the position angles of the roughly linear structures traced by the masers indicate that the 321 GHz masers are along the jet while the 22 GHz masers are perpendicular to it. We interpret the submillimeter masers in Cepheus A to be tracing significantly hotter regions (600–2000 K) than the centimeter masers.

Subject headings: ISM: individual (Cepheus A) — ISM: jets and outflows — masers — stars: formation

1. INTRODUCTION

Since its discovery in the interstellar medium nearly four decades ago (Cheung et al. 1969), the water maser emission at 22.235 GHz from the $6_{16} - 5_{23}$ transition has been extensively studied in a variety of sources, from circumstellar envelopes of late-type stars, star-forming regions and external galaxies (e.g., Elitzur 1992). This maser emission is understood to be arising from shocked gas with temperatures ~ 500 K and densities $\sim 10^9 \text{ cm}^{-3}$ (Elitzur et al. 1989).

Single-dish observations of the 22 GHz water maser emission have helped identify the early stages of massive star-formation (e.g., Sridharan et al. 2002; Brand et al. 2003). Very Large Array (VLA) and Very Long Baseline Interferometry (VLBI) observations have allowed probing of kinematics of gas in such regions with very high angular resolution of $0''.08 - 0.5$ mas (e.g., Claussen et al. 1998; Furuya et al. 2000, 2005; Patel et al. 2000; Imai et al. 2000; Torrelles et al. 2001a, 2001b; Gallimore et al. 2003; Goddi et al. 2005; Goddi & Moscadelli 2006; Moscadelli et al. 2005). However, with observations of just the 22 GHz transition alone, it remains difficult to characterize the relative differences in the physical conditions in a given star-forming region. Nearly simultaneous observations of multiple masing transitions at comparable angular resolutions would be very helpful to allow probing of physical conditions of the masing gas such as its temperature and density, beyond just the lower limits required to satisfy the maser excitation.

Except for the 22 GHz transition, and the 183.310 GHz $3_{13} - 2_{20}$ transition, other transitions of H_2O lie in the submillimeter band (Neufeld & Melnick 1991). Of

these, several submillimeter masers have been detected with single-dish observations from star-forming regions as well as late-type circumstellar envelopes (Menten et al. 1990a, 1990b; Melnick et al. 1993). Interferometric observations of some of these transitions are only now possible with the availability of the Submillimeter Array (SMA; Ho et al. 2004, Humphreys et al. 2005).⁵

Cepheus A is a well-studied high-mass star-forming region in the Cepheus OB3 complex of molecular clouds (Sargent 1977). Several compact objects in this region have been identified from radio continuum observations at centimeter wavelengths with the VLA (hereafter described as HW sources: Hughes & Wouterloot 1984; Garay et al. 1996; Martín-Pintado et al. 2005). The 22 GHz water masers have been observed towards several of these HW sources (Torrelles et al. 1996, 2001a, 2001b; Vlemmings et al. 2006) but observations of submillimeter masers have the potential of allowing a study of differences in the physical conditions in these sources, and hence may lead to a better understanding of their evolutionary differences.

Here we report the first detection of the submillimeter wavelength water maser emission in the Cepheus-A region. The fact that this emission is detected at all, suggests the presence of highly excited gas due to the very high energy levels of the submillimeter maser transitions.

2. OBSERVATIONS

The Cepheus A star-forming region was observed with the SMA on 2004 August 30 using seven antennas in the extended configuration with a maximum baseline length of 220 m. The phase center was $\alpha(2000) = 22^{\text{h}}56^{\text{m}}17.971^{\text{s}}$, $\delta(2000) = +62^{\circ}01'49''.279$. We used a tuning of 321.226 GHz to center the water maser lines in the lower sideband (LSB). The quasars BL Lac and 0102+584 were observed for 5 minutes each between every cycle of 20 minutes on the main source. The spectral band-pass was calibrated using observations of Uranus

¹ Harvard-Smithsonian Center for Astrophysics, 60 Garden Street, Cambridge, MA; npatel@cfa.harvard.edu, qzhang@cfa.harvard.edu, tksridha@cfa.harvard.edu, pho@cfa.harvard.edu.

² Instituto de Astronomía, Universidad Nacional Autónoma de México (UNAM), Mexico; scuriel@astroscu.unam.mx.

³ Academia Sinica Institute of Astronomy and Astrophysics, Taipei, Taiwan

⁴ Instituto de Ciencias del Espacio (CSIC)-IEEC, Facultat de Física, Universitat de Barcelona, Barcelona, Spain; torrelle@erupia.ieec.fcr.es

⁵ The Submillimeter Array is a joint project between the Smithsonian Astrophysical Observatory and the Academia Sinica Institute of Astronomy and Astrophysics, and is funded by the Smithsonian Institution and the Academia Sinica.

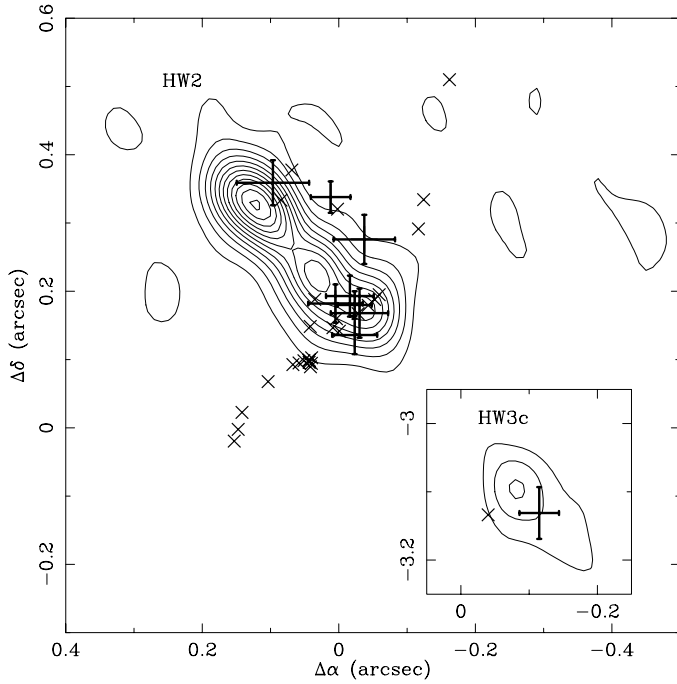


FIG. 1.— VLA map of 1.3 cm continuum emission from HW2 and HW3c (*inset*). The positions of submillimeter water masers observed with the SMA are shown with error bars representing the formal uncertainties. The position offsets were obtained by fitting two-dimensional elliptical Gaussians to integrated intensity maps over channels in which the maser emission appeared (using the IMFIT task in Miriad). The position offsets are with respect to the absolute coordinates: $\alpha(2000) = 22^h56^m17.971^s$, $\delta(2000) = +62^\circ01'49.''279$. The crosses show the positions of the 22 GHz water masers observed with the VLA (this Letter). The errors in the positions of the 22 GHz water masers are smaller than the size of the symbols shown. Only three of these centimeter wavelength masers appear to be correlated with the submillimeter masers in both position and velocity (see Table 1). Only HW2 and HW3c show the presence of submillimeter water masers among all the compact continuum sources in the entire Cepheus-A star-forming region (over $\pm 5''$). The VLA beam is $0.''09 \times 0.''07$ (P.A. 14°). The SMA beam is $0.''8 \times 0.''7$ with a P.A. of -80° .

and Saturn and absolute flux calibration was done using Neptune and the quasar 2232+117. Results from the upper sideband data (centered at 331 GHz, including CH_3CN lines and continuum emission) have been reported earlier by Patel et al. (2005). Weather conditions were excellent during the observations with relative humidity $\sim 10\%$ and $\tau_{225\text{GHz}} \approx 0.08$ ($\tau_{321\text{GHz}} \approx 0.69$), measured at the nearby Caltech Submillimeter Observatory. The track was ~ 10 hr long with on-source integration time of ~ 6.5 hr. $T_{\text{sys},\text{DSB}}$ varied from 320 to 500 K. The visibility data were calibrated using the Owens Valley Radio Observatory's MIR package and imaging was done using the Miriad package. We applied the self-calibration solutions obtained from the continuum emission (of ~ 2 Jy beam $^{-1}$) from the HW2 source obtained from the LSB data, to the spectral-line data of the submillimeter wavelength water masers. With uniform weighting, the synthesized beam was $0.''8 \times 0.''7$ with a position angle (P. A.) of -80° . We expect the maximum error in our absolute astrometry to be $\sim 0.''1$, based on positions of quasars mapped in our SMA observations. We estimate an uncertainty of $\sim 20\%$ in the absolute flux scale in the SMA data.

We also observed the 22.235 GHz water masers in

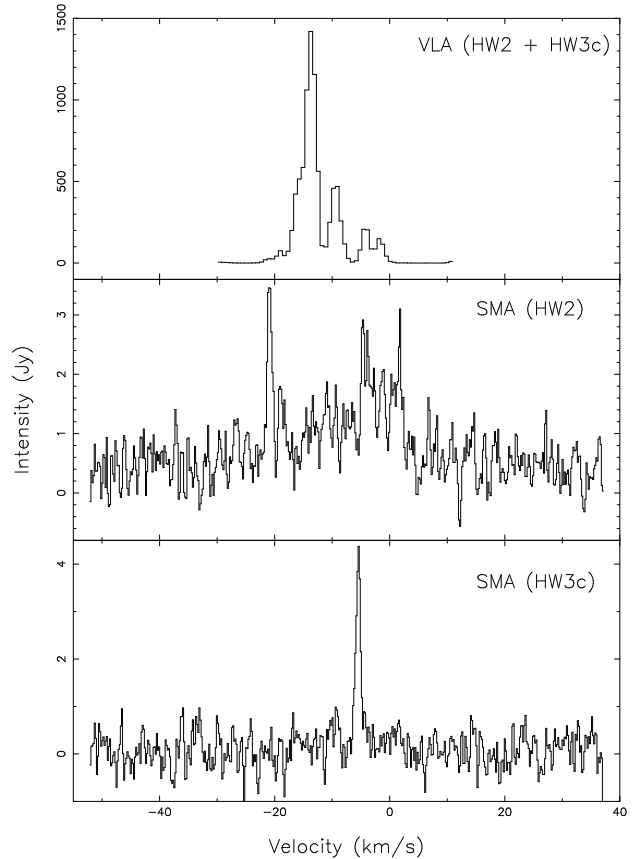


FIG. 2.— Spectra of submillimeter and centimeter wavelength water maser emission from Cepheus A HW2 and HW3c.

Cepheus-A with the VLA of the NRAO⁶ in the A configuration on 2004 October 12. These observations were made in snapshot mode with a total integration time of about 15 minutes on-source. The rms noise level in our VLA observations is about 3.3×10^{-3} Jy beam $^{-1}$ in channels free of maser emission and $\sim 4.5 \times 10^{-1}$ Jy beam $^{-1}$ in the channel with the strongest maser spot. The line and continuum data at 1.3 cm were obtained simultaneously and the astrometric registration between the maser and continuum emission is better than $0.''01$. These data were reduced using the NRAO AIPS package.

3. RESULTS

Maps of the 1.3 cm continuum emission observed with the VLA (on 2004 October 12), with an overlay of the 22 GHz water masers and the 321 GHz water masers observed with the SMA are shown in Figure 1. The 321 GHz water masers were detected only in HW2 and HW3c. The HW2 thermal jet has been observed earlier in several epochs from 1991 to 2004 and proper motions of ~ 500 km s $^{-1}$ of this jet were recently reported by Curiel et al. (2006). The position angle of the jet of $\sim 45^\circ$ is nearly perpendicular to the proposed circumstellar disk seen as a flattened elongated structure in continuum emission at $900 \mu\text{m}$ and CH_3CN line emission (Patel et al. 2005). A large majority of the 22 GHz masers are roughly along the direction of the disk (which is a larger structure of $1''$ beyond the scale of Fig. 1), consistent with

⁶ The National Radio Astronomy Observatory is a facility of the National Science Foundation operated under cooperative agreement by Associated Universities, Inc.

that found earlier by Torrelles et al. (1996, 2001a, 2001b) in their VLA and Very Long Baseline Array (VLBA) observations. The 321 GHz masers in HW2 appear to lie along the outflow jet. A total of 39 masers were detected at 22 GHz, only those associated with HW2 and HW3c are shown in Fig. 1.

Figure 2 shows the spectra of 22 and 321 GHz masers in HW2 and HW3c. With respect to the systemic velocity of the ambient molecular cloud in Cepheus A ($V_{LSR} \simeq -11 \text{ km s}^{-1}$; Gómez et al. 1999), the strongest emission in submillimeter masers associated with HW2 appears to occur at relatively higher velocities, whereas the 22 GHz masers are significantly weaker at these velocities. The brightest 22 GHz masers have flux density of $\sim 1400 \text{ Jy}$, while the brightest 321 GHz maser is $\sim 4 \text{ Jy}$. The 22 GHz masers are about a factor of 1000 times brighter than the 321 GHz masers in general. The observed characteristics of the submillimeter masers are listed in Table 1 along with corresponding values for the three spatially and kinematically associated 22 GHz masers.

4. DISCUSSION

From the sizes of the 321 GHz emission spots in channel maps and the observed flux densities, we estimate a lower limit in the brightness temperature to be $\sim 200 \text{ K}$. Since we do not have a reliable estimate of the sizes of these spots, we are unable to check whether the emission is due to maser action based on the brightness temperature. The narrow line-widths of the 321 GHz emission ($0.3\text{--}1 \text{ km s}^{-1}$) compared to the widths of the CH_3CN lines, strongly suggest that the 321 GHz lines are indeed due to maser emission.

The first astronomical detection of the $10_{29} - 9_{36}$ transition of H_2O masers was made by Menten et al. (1990a) with the Caltech Submillimeter Observatory 10.4 m telescope. Shortly after the discovery of the 321 GHz masers, Neufeld & Melnick (1990, hereafter, NM90), showed that the observed 22 and 321 GHz masers can be explained by collisional excitation within the same volume of gas. NM90 presented models of the emissivity ratio R of 22 GHz / 321 GHz maser luminosities as a function of ξ and T , where ξ is a combination of parameters involving the gas density, abundance of water and the magnitude of velocity gradient in the slab of gas that is masing (see equation 1 of NM90). In a subsequent paper, Neufeld & Melnick (1991) presented more detailed theoretical calculations including 349 rotational states of ortho and para water under a range of ξ and radiation field. The 321 GHz transition is among the 20 other theoretically predicted maser transitions in the frequency range of 183–1542 GHz. Many of these transitions are shown to be approaching in brightness to the 22 GHz maser, under certain ranges of T and ξ . Yates et al. (1997) carried out similar calculations for several submillimeter H_2O maser transitions, including the 321 GHz line. Their range of physical conditions is wider than in NM90 and Neufeld & Melnick (1991), and they also considered the effects of radiation from dust grains. According to these models, the 321 GHz maser is strongly inverted under more restricted conditions than the 22 GHz line (see Fig. 3 of NM90 and Fig. 4a of Yates et al. 1997). In fact, strong inversion of the 321 GHz transition requires $T_k > 1000 \text{ K}$. Assuming a temperature of 1400 K, the greatest gain in the 321 GHz line occurs for gas density $n(\text{H}_2)$ in the

range of $4\text{--}6 \times 10^8 \text{ cm}^{-3}$ (Yates et al. 1997).

All of these model calculations have a central assumption that the submillimeter and centimeter wavelength masing transitions arise in the same volume of gas. This implies that the 22 GHz masers have a broader range of physical conditions in temperature and densities (Yates et al. 1997). (There can be 22 GHz emission and no accompanying 321 GHz masers in the same region but not vice-versa, according to these models). We can confront these models with our maps of 22 and 321 GHz masers, to first ask if these masers arise in the same volume of gas, and if they do, what are the implications of the observed luminosity ratio.

Figure 1 and Table 1 show that we have two out of eight masers in HW2 that appear to be coincident in both spatial and velocity neighborhood ($< 0.''1$ and $< 3 \text{ km s}^{-1}$) with 22 GHz masers. In addition, we have one more region in the HW3c which is located $\sim 3''$ south of HW2, that appears to have masers at both 22 GHz and 321 GHz arising from the same region. If we use a more stringent criteria for coincidence of masers in line-of-sight velocity to be within 1 km s^{-1} , based on the typical line widths of the maser emission, we would have only one maser spot (occurring in HW3c; number 9 in Table 1) that would be coincident. The coincidence of masers 1 and 7 in HW2, might therefore be considered to be tentative, given the larger difference in their velocities. We speculate that this difference in velocity is related to the fact that HW2 is a dynamically more active region compared to HW3c.

The emissivity ratio R (22/321 GHz) for these masers listed as numbers 1, 7, and 9 in Table 1 are 9.2, 0.02, and 0.18. The value of R is roughly expected to decrease with temperature, given that $E/k = 643 \text{ K}$ for the 22 GHz transition and 1861 K for the 321 GHz line. In this way, a much hotter gas is required for the submillimeter wavelength maser excitation. Assuming that both 22 and 321 GHz masers are saturated, the luminosity ratio is then the same as the ratio of rate coefficients as defined by NM90 and plotted in their Fig. 3. We find that for maser-1 (Table 1), the observed ratio implies the kinetic temperature to be in the range of 500–2000 K, depending on the value of ξ . According to NM90, the typical value of $\log \xi$ would be in the range of -1.25 to -0.25 for the shocked gas in star-forming regions and their Figure 3 would then imply a temperature of $\sim 600 \text{ K}$ for the region where maser 1 occurs. Masers 7 and 9 have much smaller values of R , much less than 1. Even for $R = 5$, according to NM90, such masers would presumably exist behind slower non-dissociative shocks in which the kinetic temperature of the gas is $\sim 1000 \text{ K}$. Again, according to figure 3 of NM90, this value of $R < 1$ implies gas temperatures as high as 2000 K for a wide range of ξ .

With respect to the remaining six masers (listed as numbers 2–6 and 8 in Table 1) that show emission only in the 321 GHz and not in the 22 GHz transition, we cannot apply any of the existing theoretical models to these $R \rightarrow 0$ cases that imply that the 22 GHz masers are quenched but the 321 GHz emission remains strong. According to Figure 3 of NM90, which has the lowest contour corresponding to $R = 1.5$, the regions with $R \rightarrow 0$ may imply temperatures greater than 2000 K. On the other hand, we cannot completely rule out the effect of time variability for the absence of 22 GHz masers corre-

sponding to some the observed 321 GHz masers.

The 22 GHz masers are well known to be time-variable. Previous VLBA observations of Cepheus A (Torrelles et al. 2001a, 2001b) and IRAS 21391+5802 (Patel et al. 2000), show that several masing spots disappear over timescales of 1 month. These masers however, tend to be relatively weaker. The theoretical models as in NM90 predict strong emission at 22 GHz corresponding to the 321 GHz masers. If these corresponding 22 GHz masers existed during the epoch of the submillimeter observations, they are unlikely to have been completely extinguished about a month later in the centimeter wavelength observations.

Much less is known about the variability of the 321 GHz masers. In late-type stars, near simultaneous observations of 22, 321, and 325 GHz masers were carried out by Yates & Cohen (1996) over four epochs separated by ~ 20 days. They find the 321 GHz masers to be the most variable, in terms of both changes in brightness – by a factor of 2 – 10 and the shortness of time scale, by ~ 20 days. However, it remains unclear how far we can carry forward these findings to the case of water masers associated with star-forming regions.

The 22 GHz masers that are not associated with the 321 GHz masers are likely to be arising in relatively cooler regions among the various HW sources in Cepheus A, compared to HW2 and HW3c. The fact that the submillimeter wavelength masers in HW2 are found along the major axis of the jet, lead us to propose that they are arising in hotter gas regions due to the impact of the jet.

5. CONCLUSIONS

We report the first detection of 321 GHz water masers in the high-mass star-forming region Cepheus A. The

SMA observations at $\sim 0.''8$ have sufficient spatial resolution to allow a study of the association of these masers with the multiple radio continuum sources such as HW2 and HW3c (separated by about $3''$), and also with the disk-outflow system of HW2 which has a size scale of about $1''$ (725 AU). We had near-simultaneous 22 GHz water maser observations made with the VLA that show, in general, a poor agreement between the locations of submillimeter and centimeter water masers: only three out of nine masers agree in both position and line-of-sight velocities. Moreover, the submillimeter masers are found to lie along the outflow jet whereas the 22 GHz masers are primarily found perpendicular to it. The mapping of submillimeter wavelength masers with the SMA, along with near-simultaneous mapping of the 22 GHz water masers with the VLA, opens the possibility of studying the physical conditions of density and temperature of the gas associated with high-mass star-forming sites (where conditions are likely to be suitable for excitation of submillimeter water masers), at very high spatial resolution (~ 100 AU).

It is a pleasure to thank James Moran, Gary Melnick, David Neufeld and Elizabeth Humphreys for helpful discussions. We are grateful to the SMA staff in Cambridge, Hilo and Taipei, for their help with observations. We thank the referee for helpful comments on the manuscript. SC acknowledges support from DE-GAPA/UNAM and from CONACyT (México) grant 43120–F. JMT acknowledges partial financial support from the Spanish grant AYA2005-08523-C03.

REFERENCES

- Brand, J., Cesaroni, R., Comoretto, G., Felli, M., Palagi, F., Palla, F. & Valdetaro, R., 2003, *A&A*, 407, 573
- Cheung, A. C., Rank, D. M., Townes, C. H., Thornton, D. D., & Welch, W. J., 1969, *Nature*, 221, 626
- Claussen, M. J., Marvel, K. B., Wootten, A., & Wilking, B. A., 1998, *ApJ*, 507, L79
- Curiel, S., et al. 2006, *ApJ*, 638, 878
- Elitzur, M., Hollenbach, D. J., & McKee, C. F., 1989, *Ap. J.*, 246, 983
- Elitzur, M., 1992, *Astronomical Masers* (Dordrecht: Kluwer)
- Furuya, R. S., Kitamura, Y., Wootten, H. A., Claussen, M. J., Saito, M., Marvel, K. B., & Kawabe, R. 2000, *ApJ*, 542, L135
- Gallimore, J. F., Cool, R. J., Thornley, M. D., & McMullin, J. 2003, *ApJ*, 586, 306
- Goddi, C., & Moscadelli, L. 2006, *A&A*, 447, 577
- Goddi, C., Moscadelli, L., Alef, W., Tarchi, A., Brand, J., & Pani, M. 2005, *A&A*, 432, 161
- Gómez, J. F., Sargent, A. I., Torrelles, J. M., Ho, P. T. P., Rodríguez, L. F., Cantó, J., & Garay, G., 1999, *ApJ*, 514, 287
- Hughes, V. A. & Wouterloot, J. G. A., 1984, *ApJ*, 276, 204
- Ho, P. T. P., Moran, J. M. & Lo, K. Y., 2006, *ApJ*, 616, L1
- Humphreys, E. M. L., Greenhill, L., Reid, M., Beuther, H., Moran, J., Wilner, D., Kondratko, P., 2005, *ApJ*, 634, L133.
- Imai, H., Kameya, O., Sasao, T., Miyoshi, M., Deguchi, S., Horiuchi, S., & Asaki, Y. 2000, *ApJ*, 538, 751
- Martín-Pintado, J., Jiménez-Serra, I., Rodríguez-Franco, A., Martín, S., Thum, C. 2005, *ApJ*, 628, L61
- Menten, K. M., Melnick, G. J., & Phillips, T. G., 1990, *ApJ.*, 350, L41
- Menten, K. M., Melnick, G. J., Phillips, T. G. & Neufeld, D. A., 1990, *ApJ*, 363, L27
- Melnick, G. J., Menten, K. M., Phillips, T. G. & Hunter, T., 1993, *ApJ*, 416, L37
- Moscadelli, L., Cesaroni, R., & Rioja, M. J. 2005, *A&A*, 438, 889
- Neufeld, D. A., & Melnick, G. J., 1990, *Ap. J.*, 352, L9 (NM90)
- 1991, *Ap. J.*, 368, 215
- Patel, N. A., Greenhill, L. J., Herrnstein, J., Zhang, Q., Moran, J. M., Ho, P. T. P., & Goldsmith, P. F., 2000, *ApJ*, 538, 268
- Patel, N. A., et al. 2005, *Nature*, 437, 109
- Sargent, A. I. 1977, *ApJ*, 218, 736
- Sridharan, T. K., Beuther, H., Saito, M., Wyrowski, F. & Schilke, P., 2002, *ApJ*, 566, 931
- Torrelles, J. M., Gómez, J. F., Rodríguez, L. F., Curiel, S., Ho, P. T. P., & Garay, G., 1996, *ApJ*, 457, L107
- Torrelles, J. M., et al. 2001a, *ApJ*, 560, 853
- 2001, *Nature*, 411, 277
- Vlemmings, W. H. T., Diamond, P. J., van Langevelde, H. J., & Torrelles, J. M., 2006, *A&A*, 448, 597.
- Yates, J. A., & Cohen, R. J., 1996, *MNRAS*, 278, 655.
- Yates, J. A., Field, D., & Gray, M. D., 1997, *MNRAS*, 285, 303.

TABLE 1
SUMMARY OF DETECTED MASERS

No.	321 GHz MASERS ^a				22 GHz MASERS ^b			
	$\Delta\alpha$	$\Delta\delta$	Flux Density	V_{LSR}	$\Delta\alpha$	$\Delta\delta$	Flux Density	V_{LSR}
	"	"	(Jy)	(km s ⁻¹)	"	"	(Jy)	(km s ⁻¹)
1	0.096	0.359	2.8	-19.0	0.068	0.378	25.9	-21.1
2	0.012	0.338	4.8	-21.0
3	-0.037	0.276	2.9	-11.0
4	-0.016	0.193	2.7	-4.5
5	0.005	0.182	3.0	-1.0
6	-0.023	0.180	6.5	-3.5
7	-0.030	0.168	5.1	1.2	-0.004	0.167	0.09	4.0
8	-0.023	0.136	1.7	-3.8
9 ^c	-0.115	-3.131	3.7	-5.5	-0.005	-3.133	0.67	-5.6

^a Typical uncertainty in SMA flux values is 0.4 Jy. Formal uncertainty in Gaussian fitted positions is ~ 30 mas (see error-bars on position offsets showned in Fig. 1).^b The 22 GHz masers listed here are a subset of all the masers detected in the VLA observations. Only those masers which are most likely to be associated with the 321 GHz masers (closest occurrences in position and velocity) are tabulated here. Typical uncertainty in VLA flux values is 10 mJy and formal uncertainty in positions is ~ 1 mas.^c This maser is associated with HW3c, all others are associated with HW2.